EFFECT OF *Arx*$^{(GCG)7}$ MUTATION IN THE OLFACTORY BULB

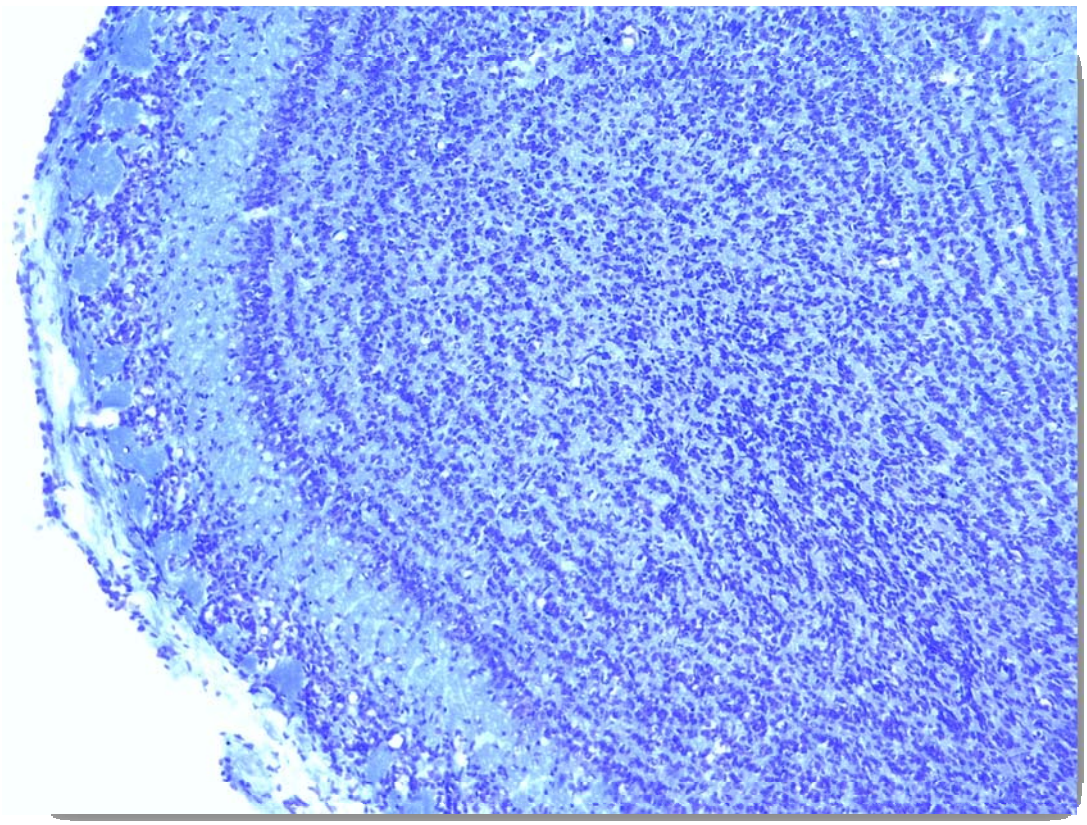

AMALIA RUIZ SERRANO

SEVILLA, JUNIO 2014

UNIVERSIDAD PABLO DE OLAVIDE SEVILLA AÑO 1997

cabimer
CENTRO ANDALUZ DE BIOLOGÍA MOLECULAR & MEDICINA REGENERATIVA

GRADO EN BIOTECNOLOGÍA

PROYECTO FIN DE GRADO

ACKNOWLEDGEMENT

Foremost, I would like to express my sincere gratitude to my tutors:

- To **Dr. Manuel Álvarez Dolado** for offering me the possibility to participate in such an amazing research project in his laboratory and for allowing me to grow as a research scientist. I deeply appreciate his continuous advices, mentorship and patience with me in the lab. As well as his recommendations on my career.

- To **Prof. Ana Moral Rama** for having been there since the beginning. She has always offered continuous support to allow me doing a research project that I really like. Her confidence in my work has been priceless, encouraging me every single moment.

My sincere thanks also to **Maleles Martínez Losa** and **Cindy Cruz Zambrano**, who helped and gave me their best suggestions, while at the same time teach me lab skills. Also, thanks for spreading happiness on those scientifically hard days.

I want to thank to my fellow labmates **Marina**, **Jesús**, **Olga**, **Michele** and **Enrico** for providing great friendly atmosphere and sharing with me their experiences.

Last but not least, I would like to thank my family. In particular, the unconditional patience and understanding provided by my parents and brother.

Thank you all!

ABBREVIATIONS

ARX: Aristaless related homeobox

Arx$^{(GCG)}_7$: Arx with c.304ins$(GCG)_7$ mutation

Blc: Blanes cells

Cb: Calbindin

CF: Centrifugal Fibers

CR: Calretinin

Cy5: Cyanine 5

EEG: Electroencephalon

EPL: External plexiform layer

eTc: External tufted cells

FITC: Fluorescein isothiocyanate

Gc: Granule cells

GL: Glomerular layer

HcC: Horizontal cell of Cajal

iTc: Inner tufted cells

KO: Knock-out

Mc: Mitral cells

MCL: Mitral cell layer

mTc: Middle tufted cells

PBS: Phosphate buffered saline

PX: Postnatal age of X days

OB: Olfactory bulb

OE: Olfactory epithelium

ONL: Olfactory nerve layer

Pgc: Periglomerular cell

RMS: Rostral migratory stream

s.e.m.: Standard error mean

SSAc: Superficial short axon cell

SVZ: Subventricular zone

TH: Tyrosine hydroxylase

UTR: Untranslated región

vcC: Vertical cell of Cajal

vGc: Van Gehuchten cell

WMS: White matter subependymal

WS: West Syndrome

wt: Wild type

TABLE OF CONTENT

TABLE OF CONTENTS

Pgs.

Eliminado: 3

Eliminado: 3
Eliminado: 3
Eliminado: 3
Eliminado: 3

RESUMEN

1. RESUMEN

La formación de la estructura del bulbo olfativo, organizada en diferentes capas interconectadas, está finamente controlada por multitud de factores. El trabajo previo de Yoshihara et al. demostró que el factor de transcripción Arx se requiere para el correcto desarrollo del bulbo olfativo. No obstante, este grupo realizó su estudio en ratones con una mutación Knock-out para *Arx*, la cual no se encuentra de forma natural en roedores o humanos. La mutación *Arx*$^{(GCG)}_{7}$ es la mas frecuente en humanos y está relacionada con una encefalopatía epiléptica infantil denominada Síndrome de West. En el presente trabajo hemos estudiado el posible efecto de esta mutación en la morfología del bulbo olfativo para entender mejor esta patología. Los ratones macho *Arx*$^{(GCG)}_{7}$ con 18-21 dias de edad presentaron evidentes anomalías en la citoarquitectura del bulbo olfativo: (1) reducción del tamaño de la capa plexiforme interna, (2) pérdida de células periglomerulares tiroxina hidroxilasa-positivas, (3) pérdida de células periglomerulares calbindina-positivas, y (4) reducción en el tamaño de los glomérulos de la capa glomerular. Por ello, concluimos que la correcta actividad de *Arx* es esencial para la generación y diposición de las interneuronas periglomerulares del bulbo olfativo y probablemente para una adecuada inervación axonal en la capa plexiforme interna.

Palabras clave: mutación *Arx*$^{(GCG)}_{7}$, bulbo olfativo, células periglomerulares, capa plexiforme interna, Síndrome de West.

ABSTRACT

2. ABSTRACT

The olfactory bulb provides an excellent model in which neurons and their axonal connections are organized into distinct layers corresponding to different functionalities. In this project, we support the previous study of Yoshihara et al. to demonstrate that transcription factor Arx is required for olfactory bulb development. However, instead of doing the research under *Arx* Knock-out mice, we report the anomalies of *Arx*$^{(GCG)}_{7}$ mutation related to an infantile epilepsy called West Syndrome. Mice with this mutation displayed cytoarchitecture abnormalities in the olfactory bulb: (1) size reduction of the internal plexiform layer, (2) loss of tyroxine hydroxylase-positive periglomerular cells, (3) loss of calbindin-positive periglomerular cells, and (4) reduced glomeruli size in the glomerular layer. Thus, a complete activity of *Arx* contributes to olfactory bulb interneurons diversity and likely a role in regulating the expression for a proper axonal innervation in the internal plexiform layer.

Key words: *Arx*$^{(GCG)}_{7}$mutation, ofactory bulb, periglomerular cells, West Syndrome, internal plexiform layer.

INTRODUCTION

3. INTRODUCTION

3.1. Olfactory system in mice

Olfactory system is one of the main sensorial organs in rodents. In humans, also provides numerous functions, influencing in behavior, awareness of environmental hazards and social communication. The complex structure is finely organized during development. In the present work we will study the possible role of *Arx* gene on the morphological configuration of the olfactory bulb (OB). Below, its normal anatomy and circuitry will be described.

3.1.1. Morphology and circuitry of OB

The olfactory system is phylogenetically ancient, close to the periphery of the brain and is supposed to be a precursor for higher parts of the brain (Pahle et al., 2000).The first relay station in the olfactory system is OB, where odor information is transferred from the periphery to higher centers in the brain. Different types of neurons and glia are disposed in a precise structured layer organization.

The following layers are distinguished in the OB, from the outer to the inner zone (**Figure 1**):

- Olfactory nerve layer (ONL): it contains olfactory ensheathing glia that enwraps amielinic axons projected by nerve fibers from the olfactory epithelium (OE).
- Glomerular layer (GL): formed by glomeruli, spherical structures with a high quantity of neuropil surrounded by periglomerular and glial cells. Synapses occur in glomeruli with primary dendrites of projection neurons from the ONL, ML and dendrites of interneurons.
- External plexiform layer (EPL): it presents bodies of tufted cells which are considered projection neurons. In this zone extensive interaction occurs between the apical dendrites of granule cells and the lateral dendrites of granule cells and the lateral dendrites of mitral cells.
- Mitral cell layer (MCL): formed by bodies of mitral cells, which are projection neurons. The apical dendrites enter glomeruli in the GL and secondary dendrites of mitral cells extend to the EPL engaging in dendrodendritic synapses with dendrites of granule cells. On the other hand, axons of mitral cells are projected into the internal plexiform layer (IPL).

- Granule cell layer (GCL): Granule cells are similar in size to periglomerular cells and also are inhibitory. Their most characteristic feature is the absence of an axon. They form complex webs of lateral inhibitory connections between mitral and tufted cells of different glomeruli. In this way, they are a powerful inhibitory influence on the output neurons of the OB. In the GCL there are also migrating immature interneurons from the rostral migratory pathway to the periglomerular area. These immature neurons are ensheathing by astrocytes and differentiate local interneurons (Yoshihara et al., 2005).

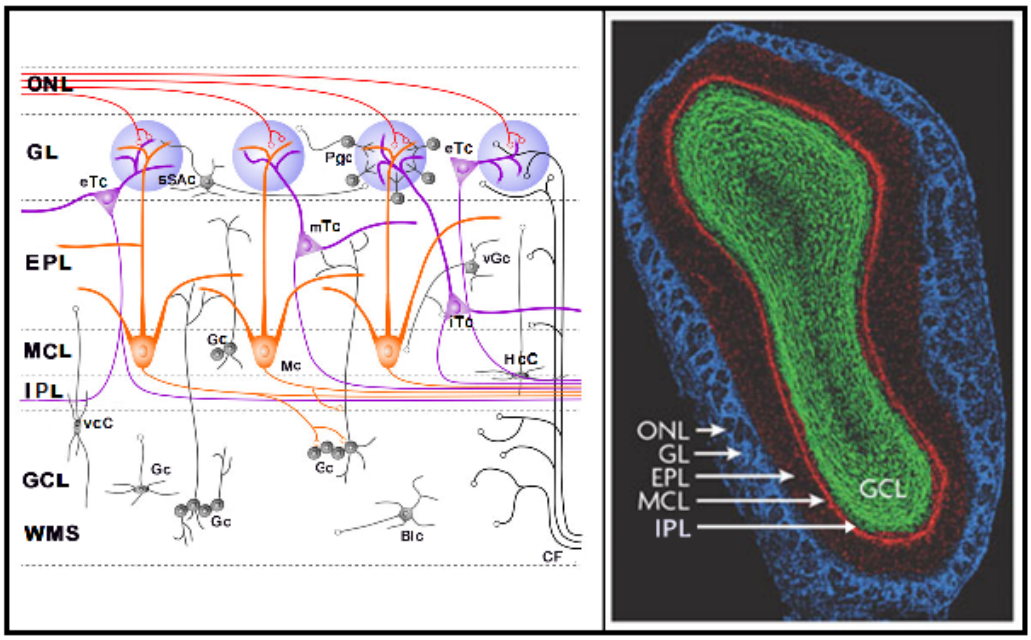

- Figure 1: Olfactory bulb in rodent.

Left: laminar organization of the olfactory bulb. From the upper to the lower zone we appreciate the following layers with their correspondent cells: ONL (olfactory nerve layer); GL (gromerular layer) with external tufted cells (eTc), superficial short axon cell (SSAc), periglomerular cell (Pgc); EPL (external plexiform layer) with middle Tufted cells (mTc), van Gehuchten cell (vGc), inner tufted cells (iTc); MCL (mitral cell layer) with granule cells (Gc), mitral cells (Mc), horizontal cell of Cajal (HcC); IPL(internal plexiform layer)with the axons of the proximal layers; GCL (Granule Cell Layer) with vertical cell of Cajal (vcC), Gc, Blanes cells (Blc) and centrifugal fibers (CF); white matter subependymal (WMS). **Right**: Cross section of the olfactory bulb where olfactory sensory neurons (OSNs) cover the outermost layer of the bulb forming the ONL. These axons enter the glomeruli branching and forming synapses with second-order projection neurons in the GL (blue). It is surrounded by interneuron cell bodies in the EPL(light red) where extensive interaction occurs between the apical dendrites of granule cells and the lateral dendrites of granule cells and the lateral dendrites of a thin band of mitral cell bodies (bright red). Axons converge in the IPL (black) and finally in the center lies the GCL with migrating immature interneurons (green). Left diagram is a modification of Puche, 2003 (http://www.apuche.org/OIA/) and right image is taken from Zou et al., 2009.

Regarding the odor essence circuitry (**Figure 1**), odorants are perceived by chemoreceptors in the olfactory epithelium, located in the roof of the two nasal cavities. There are four olfactory receptor neurons which receive the signal and transmit it through the olfactory nerve layer to a specific glomerulus. Here, excitatory synaptic connections on dendrites of mitral and tufted cells take place and is transferred through their axons to the olfactory cortex. The signal will be directly send to the higher levels of the central nervous system in the corticomedial amygdala portion of the brain where the information is decoded, interpreted and answered (Mori et al., 1999). It must be highlighted the complex synapses occurred in the OB, which is classified in three main categories of neurons. The first category is integrated by principal cells, mitral and tufted cells, constituting typical axon-dendritic synapse and atypical dendro-dendritic/somato-dendritic reciprocal synaptic contacts with interneurons. The second category include granule, periglomerular and most of the interneurons cells located in the EPL, engaged in dendrodendritic reciprocal synapses with principal cells and a high percentage of anaxony. The third one is integrated by short-axon cells with axons and do not innervate principal cells (Crespoet al., 2003).

OB morphogenesis consist in two steps: firstly, differentiated projection interneurons are accumulated at the anterior tip of telencephalon and secondly, further expansion of massive differentiated interneurons is produced along their lifespan. We should also take into account that projection neurons are born earlier than the interneurons and that the latter are continuously generated. The interneurons progenitors are born in the subventricular zone (SVZ) of the cerebral cortex and migrate via the rostral migratory stream (RMS) toward the OB (Yoshihara et al., 2005).

To determinate the previously described structured layer morphology, a gene network and a pleyade of factors should perform their correct function in a precise time. Among these genes, we will outline the function of *Arx* gene, described below.

3.2. *Arx* gene

Arx (*Aristaless related homeobox*) is a paired class homeobox gene located on human chromosome Xp22.13, so it is expressed during development. It is a small gene of ~12.5kb with five exons encoding for a protein of 562 amino acids. Additionally, in the brain and

skeletal muscle it has a ~2.8 kb transcript, while it has larger isoforms in the heart and others shorter in the skeletal muscle. Alternative splicing within the coding region is unlikely due to its preservation, just presenting isoforms as a consequence of alternative polyadenylation sites changing the size of 3' untranslated region (UTR).

Arx protein contains two conserved domains, a C-peptide or Aristaless domain and the prd-like class homeobox domain. While the Aristaless domain is supposed to be an activator domain, the homeodomain is considered as a repressor domain. Arx is a member of the group-II Aristaless-related protein family whose members are expressed primarily in the central and/or peripheral nervous system (NCBI, 2014; Gécz et al. 2006). The expressed protein has four polyalanine tracts in which 7-16 alanine residues are sequentially repeated, three of them are encoded in exon 2, and of the first and second polyalanine tracts are mutations hot spots causing mental retardation and epilepsy including West syndrome (Kato, 2006).

3.2.1. Functions

Arx belongs to a large family of homeodomain transcription factors involved in the development of testes, pancreas and forebrain. It is a pleitropic gene implicated in a wide spectrum of X-linked neurological disorders. One of them is West syndrome (WS) or Infantile Spasms Syndrome, a type of epilepsy that occurs in 2 to 3.5/10.000 live births, with onsets during the first year of life in 90% of those affected. WS is a severe epilepsy syndrome characterized by the triad of mental retardation, interictal electroencephalogram (EEG) pattern termed hypsarrhytmia and infantile spasms. The poorly characterized biological function/s made one of the reasons why is so relevant to understand the mechanism in which this gene acts. (Engel JR & Pedley, 2008; Wheless et al., 2012). In recent years, Arx protein has been described to be highly expressed in GABA interneurons, being important for their tangential migration from the ganglionic eminences to the cortical fields (Beguin et al., 2012; Gécz et al., 2006). The generation of several mouse models with KO or hypomorphic mutations has helped to better understand the functions of Arx.

3.2.2. Animal models

Arx gene was firstly studied in zebrafish and mice on the basis of its similarity to the *Drosophila* gene *Aristaless*. In 2002, the human orthologous was discovered as a result of the identification of *Arx* gene mutations in patients with WS, Partington syndrome, X-linked lissencephaly with ambiguous genitalia, X-linked myoclonic epilepsy with generalized spasticity and intellectual disability and non-syndromic X-linked mental retardation (Gécz et al., 2006).

There are a wide number of model animals with *Arx* human homologues, compiling the more significant models and evaluating their alignment sequences with NCBI database (it scores according to BLOSUM matrix) the following data is obtained:

Table 1: Aminoacidic sequence comparison between model organisms with Arx gene

Organism	Max. score	Query cover	E value	Max ident	Accession number (UniProt	Accession number (NCBI)	Length	Common name
Homo sapiens**	109	100%	0.0	100%	Q96QS3	NP_620689.1	562	Human
Otolemur garnettii*	102	100%	0.0	95%	H0XRJ8	XP_003791968.	533	Small-eared galago
Macaca mulatta*	100	100%	0.0	92%	F7HF24	XP_001091313.	562	*Rhesus macaque*
Rattus norvegicus**	788	100%	0.0	92%	A6YP92	NP_001093644.	566	Rat
Mus musculus**	755	100%	0.0	93%	O35085	BAA85852.1	564	Mouse
Oryctolagus cuniculus *	664	76%	0.0	98%	G1U424	XP_002720021.	529	Rabbit
Bos mutus	551	100%	0.0	98%	L8IVE1	XP_006990189.	503	Yak
Danio rerio**	387	94%	2e-125	78%	O42115	NP_571459.1	453	Zebra fish

. (*) They are predicted sequences, which mean that even being sequenciated, it has been predicted to be an open reading frame. (**) The sequences have been manually confirmed with Swiss- Prot database.

Mouse was selected not just because of its sequence similarity, but also for the existence of an *Arx* polyalanine mutation which simulate an analogous response in human with WS. In this way, the data obtained at the end of this study could be used in understanding the effect of *Arx* in WS.

3.2.3. Arx Polyalanine Expansion

Seven X-linked disorders involving mental retardation are associated with more than 59 mutations in the *Arx* gene: X-linked WS, Partington syndrome, X.linked lissencephaly with ambiguous genitalia, X-linked myoclonic epilepsy with generalized spasticity and intellectual disability and non-syndromic X-linked mental retardation. This variety of phenotypes is related with the position of the mutation and the consequences that have on gene expression and Arx transcriptional activity. Most of the mutations are located in exon 2 and are related with polyalanine expansions. In Arx there are 4 tracts of polyalanines. In this study we are going to focused on the c.304ins$(GCG)_7$ mutation (insertion of 7 alanines into the normal 10 alanine tract in exon 2) that cause aggregation predominately in the cytoplasm. As a phenotype it presents a lower quantity of Arx protein and an alteration of its activity as transcription factor, being proportional the number of extra alanines to the alteration in Arx protein (Gécz et al., 2006).

Mice with *Arx*$^{(GCG)}_7$ mutation displayed intense seizures and impaired learning performance. At the same time, *Arx*$^{(GCG)}_7$ mutated gene present a wide variety of biological effects according to the area of the cerebrum. In mutants an important reduction in the number of GABAergic and cholinergic neurons in the striatum, cortex, medial septum and ventral forebrain nuclei compared with wt mice. In addition, *Arx* gene has been discovered to play an important role in the correct OB development, since its complete loss cause a remarkable reduction in its size and morphologically differences. These alterations would be described better in the next section.

3.3. *Arx* homeobox gene in OB development

To understand the role of *Arx* in the development of the olfactory bulb, Yoshihara et al used *Arx* KO mice and compared the results with wild-type. This research showed significant results from where was concluded that Arx protein is expressed strongly in the interneurons and weakly in the radial glia of the olfactory bulb, but neither the olfactory sensory neurons nor bulbar projection neurons.

Arx-deficient mice showed the following abnormalities:

- Reduction in the size of the olfactory bulb.
- Interneuron progenitors reduced proliferation and impaired entry into the olfactory bulb. RMS contains migrating OB interneurons progenitors; however, they stalled at the rostral tip of the stream without entering into the OB. Most of the GABA-positive neurons could not enter and accumulated at the rostral end of the RMS and ventrally apposing region.
- Periglomerular cells expressing tyrosine hydroxylase were lost.
- Layer structure in the OB was disorganized.
- Abnormal axonal termination of the olfactory sensory neurons in an unusual axon-tangled structure (fibrocellular mass).

With these results they conclude that *Arx* is required for the development of interneurons and the establishment of functional olfactory neural circuitry by affecting Arx-non-expressing sensory neurons and projection neurons, such as regulating the expression of putative instructive signals from the OB to a properly innervation of olfactory sensory axons (Yoshihara et al., 2005).

This project is based on this research, focusing on the *Arx* mutation c.304ins$(GCG)_7$ that has been developed by Kunio Kitamura as a mouse model for the most common mutation in Arx that lead to WS.

In addition, *Arx*-deficient mice die soon after birth so the previous analysis used only male embryos until the day of birth. In contrast, *Arx*$^{(GCG)}_7$ mice are able to live until approximately 20 days. In this way we will study the anomalies in in young adult male mice. Since Arx knock-out humans and mice are not born alive, this project will allow us to determining whether there is a correlation with Yoshivara et al. and study a putative effect on the OB

formation in a mouse model that recapitulate more precisely a pathology in humans, such as WS .

HYPOTHESIS

4. HYPOTHESIS AND OBJECTIVES

West syndrome is a severe infantile epilepsy syndrome that affects 2 to 3.5/10.000 live births humans. One of the genes related to this syndrome is *Arx*, that is linked to X chromosome. Several studies have been carried out in mice to detect its role in diverse biological processes and organ development. As it has been demonstrated by Yoshivara et al., the olfactory bulb morphology differs between *Arx*-KO and wild type mice. However, individuals with a lack of function of this gene are born dead in mice as well as in humans. Therefore, it is unknown whether adult-juvenile individuals present olfactory anomalies.

In this project we will focused on *Arx*$^{(GCG)}_{7}$ mutants mice, which recapitulate the gene alterations presented in born children with WS. In order to understand better this disease and to find a possible defect in the olfactory system of WS patients, we will analyze morphologically the OB of *Arx*$^{(GCG)}_{7}$ mutant mice. We propose the working hypothesis that mutants will display anomalies in the OB morphology.

With this hypothesis we set the following objective:

- To determine the effect of *Arx*$^{(GCG)}_{7}$ gene mutation in the morphology of the OB.

In order to achieve this objective we set the goals that are listed below:

- Nissl staining to label cell layers and structural disposition of the OB as a way to show its general morphology.
- Immunohistochemistries labelling CR^{+}, Cb^{+}, TH^{+} and $Reelin^{+}$ cells to identify specific cell population of the OB and analyze their location and quantity along their specific layer distribution in 17-21 days old mice.

MATERIALS AND METHODS

5. MATERIALS Y METHODS

5.1. Animals

Mus musculus (*Muridae, Rodentia, Mammalia*) *Arx*$^{(GCG)}_7$ mutants, linked to X chromosome, in C57BL/6J background where obtained from Dr. J. Golden of the Children´s Hospital of Philadelphia (USA), and originally generated in Dr. Kitamura´s lab. Control wild type mice in C57BL/6J (JAX 000664) background were obtained from Charles River (Barcelona, Spain). Both were kept under standard conditions with cycles of 12 hours of darkness and 12 hours of light. The administration of food and water was *ad libitum*. Environmental conditions were fixed at 22±1ºC and 55±10% of humidity. The maximum of animals in each jail of polyetherimide (435 cm^3) were of 5 individuals under positive pressure ventilation and HEPA filters. A sentinel program was followed as an environmental and sanitary control. All animal procedures were carried out in accordance with the Spanish legislation (RD 1201/05 and L 32/07) and the directives of "Comité de Experimentación Animal del CABIMER".

Studied litters were generated by breeding heterozygous females (*Arx*($^{GCG}_7$/X) with wild type C57BL/6J males. Wild type males progeny (X/Y) were selected as controls and males carrying the mutation (*Arx*$^{(GCG)}_7$ /Y) were the center of our research as Arx deficient mice.

A total number of 11 animals (17-21 postnatal days) from four crossings were used in this study. Between them seven were wild type and four mutants.

5.2. DNA extraction and genotyping

DNA for genotyping was isolated from tail mice. Approximately 0.5 cm of tissue was hydrolyzed in 450µl of lysis buffer (1% SDS 20%; 10% Tris Buffer 1M pH 8,0; 1% EDTA 0,5 M; 8% NaCl 2,5M; 80% H_2O Mq) with proteinase K (Invitrogen, Carlsbad, USA). It was incubated overnight at 55°C to separate RNA y DNA with saline precipitation. The debris was removed by centrifuging for 3 min at maximum speed. 450 µl of isopropanol were added

to the sobrenatant and shaked until distinguish DNA. Another centrifugation of 10min at maximum speed was carried out washing the pellet with 450 µl of ethanol 70%. Finally, the pellet was dried and resuspended in water.

The genotype was determined with a qualitative PCR (43,4% Braun water, 20% green buffer 5x, 10% dNTPs Roche (Basel, Switzarland) 2mM, 8% $MgCl_2$ Promega (Madison, USA) 25mM, 4% DMSO Sigma-Aldrich (St. Louis, USA), 2% G7fwd TIB Mowiol Merck (Darmstadt, Germany), 2% G7rev TIB Mowiol Merck (Darmstadt, Germany), 2% kita-Neo TIB Mowiol Merck (Darmstadt, Germany), 0,6% Go Taq Promega (Madison, USA) 5U/µl, 8% DNA sample). The ARX open reading frame (ORF) spanned 1686 bp and had a 72,5% GC content , which was considered to be an unusually high content. That was the reason why DMSO was used to decrease melting temperature.

The PCR protocol consisted in:

Denaturation (1 cycle):

5 min at 94°C

Annealing (35 cycles):

30 seg at 94°C

1 min at 62°C

1 min at 72°C

Elongation (1 cycle):

5 min at 72°C

∞ at 4°C

The following primers were used:

G7Fwd (GCG7 Forward): 5'- AAA GGC GAA AAG GAC GAG GAG GAA AGG-3'

G7Rev (GCG7 Reverse): 5'-CTT TAG CTC CCC TTC GCA CAC-3'

Kita-Neo: 5'-TGT TCA ATG GCC GAT CCC AT-3'

An electrophoresis was used to separate amplified DNA fragments by size. The expected band size for wt X chromosome is 250pb and for mutant Arx^{GCG7} is 400pb and 500 pb. We should take into account that there must be three controls (+C, -C, 0C) and the molecular weight to assess the correct work of the PCR. In the following figure (Fig.2) different mice genotypes are displayed:

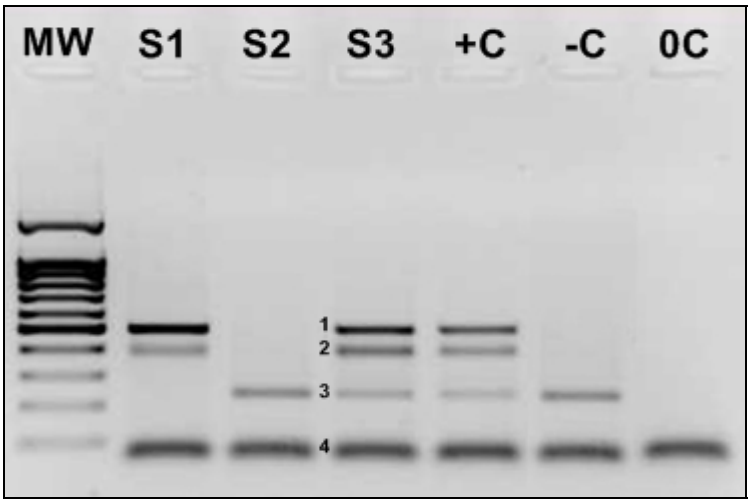

Figure 2: Gel electrophoresis picture.

MW: molecular weight, S1: sample 1 (mutant male), S2: sample 2 (wt female), S3: sample 3 (heterozygote female), +C: positive control from a ArxGCG7/X heterozygote female, -C: negative control from wt female, 0C: zero PCR control with no DNA. (1,2) Arx mutated X chromosome. (3) wt X chromosome. (4) Small DNA fragments (primer dimmer).

The agarose gel was made with 0.8% of concentration (CONDA & Pronadisa, Madrid, Spain) in TBE 1x buffer [Tris base [Sigma-Aldrich (St. Louis, USA)], boric acid [Sigma-Aldrich (St. Louis, USA)], EDTA[Sigma-Aldrich (St. Louis, USA)] with ethidium bromide to detect the DNA with an ultraviolet (UV) transilluminator, Bio-Rad Universal Hood. Quantity One software was employed for analyzing the images and estimating each size compared to the 100 Pb molecular weight [Nippon Genetics Europe GmbH (Cultek)], testing the results.

5.3. Anesthesia

Each mouse was anaesthetized with a concentration of 5 mg ketamine/xylazine per 1 kg of mice weight (20% of ketamine [Merial, Lyon, Francia], 10% of xylazine [Bayer, Barcelona, Spain], 70% of saline [Sigma-Aldrich (St. Louis, USA)])

Xylazine is an agonist at α_2 class of adrenergic receptor, while ketamine is classified as a NMDA receptor antagonist. So, that is why they interfere with pain transmission and perception. Diluting ketamine/ xylazine combination in saline solution makes easier to accurately measure volume for injection. It may also make some drugs less irritating when injected.

5.4. Perfusion

Intracardiac perfusion was used as a rapid and uniform tissue fixation/preservation method. This procedure was obtained with paraformaldehyde 4% in phosphate buffered saline (PBS)

The protocol was performed in a fume hood under security measures (gloves, glasses and mask), due to the toxicity of PFA. The next steps show the process:

1) Perfusion pump (Masterflex L/S Cole Parmer Instrument Company) attached to perfusion set and needle were adjusted to a slow steady drip (20ml/min). Mice properly anaesthetized, without pedal reflex, were placed on the operating table with its back down. In order to facilitate the surgery appendages were securely and separately fixed with the help of needles.
2) An incision was made with scalpel through abdomen along diaphragm. Connective tissue at the bottom of diaphragm was cut with sharp scissors to allow access to rib cage. Two horizontal cuts were done through the rib cage.
3) A hemostat grabbed the sternum to open up thoracic cavity and exposed heart. From this moment the process was fast to avoid the death before the perfusion.
4) Pericardium was separated with forceps and the needle was inserted directly into the left ventricle. Right auricule was cut with scissors, diminishing momentously blood pressure because of the loss of blood.
5) The valve was released to allow slow, steady flow of 10ml of PBS until blood has been cleared from body. In this moment, the solution introduced was changed to 20ml 4% PFA. Perfusion was considered completed when spontaneous movement and lightened color of the liver were observed.
6) Needles were moved away and the animal was taken from the table to decapitate with scissors. The skin and the skull were cut and retire carefully to obtain the brain, that was placed in a vial containing 10 ml of 4% PFA and post-fixed for 24 hours at 4°C.
7) Another 24 hours were required to immerse in 10 ml of 30% saccarose solution in PBS. This step would help in the cryopreservation avoiding ice crystals.

5.5. Frozen tissue sections

With the help of a mold cerebellum was separated from the other part of the brain. The telencephalon were included with a coronal disposition in a plastic mold with OCT (Sakura, Tokyo, Japan). The mold was placed into liquid nitrogen or dry ice till the tissue was completely frozen. Afterwards, they were stored at -20ºC until sectioning. Frozen tissue block were transferred to a Cryostat (Leica CM3050S) prior to sectioning allowing the temperature of the frozen tissue block to equilibrate to the temperature of the cryostat. The tissue was sectioned coronally into 10 series of 18 µm slices on glass slides. To its preservation they were stored at -20ºC until their use.

5.6. Nissl morphological study

Nissl staining was performed with the intention to provide a general and comprehensive image of the distribution, size and morphology of neurals in the tissue. The technique does not give us any information about the ramifications of these neurons, as the dyes used (cresyl violet or toluidine blue) were acidophilus and therefore bound to ribonucleic acid included in ribosomes staining nucleus, nucleolus and rough endoplasmic reticulum ribosomes. In glial cell only nuclei were stained.

A 10th serie of slices were mounted on gelatinized slides (Microscope slide 1 mm app.76x26 mm cut edges, twin frosted, Wiegand, Germany) and allowed to dry O/N. The next day, we proceeded to staining by immersing the slide in the solution of cresyl violet dye 2% for 3 minutes. After the exposure to the dye we proceeded to rinse by immersing the slide in a bath of distilled water a few seconds. Immediately, samples were dehydrated for 1 minute in a crescent gradient of alcohol solutions (50 º, 70 º, 96 º to 100 º). Finally, slides were 2 minutes in xylene (Panreac, Barcelona, Spain) and then covered with mounting medium Mowiol (Sigma-Aldrich, St. Louis, USA).

Dried samples were observed and analyzed with a bright field microscopy (Confocal Leica microscope TCS SP5 AOBS).

1.1. Immunofluorescence technique

Immunofluorescence is based on the principle of antibodies binding specifically to antigens in biological tissues. In all of the cases it was used immunofluorescence with indirect method that involved an unlabeled primary antibody that binds to the target antigen and a labeled secondary antibody with a fluorescent tag.

Table 1 shows all the references and working dilution for the primary and secundary antibodies used:

Table 2: Information about used antibodies.

	Animal of origin	Producer	Reference	Working dilution
Primary antibodies				
Anti- Reelin	Mouse	Millipore	MAB5364	1:800
Anti-Calbindin D 28K	Rabbit	Swant	CB-38a	1:2000
Anti-Calretinin	Rabbit	Swant	CR 7697	1:2000
Anti-Tyroxine Hydroxylase	Rabbit	Chemicon International	AB152	1:1000
Secondary antibodies				
Fluorescein isothiocyanate anti-rabbit	Goat	Jackson ImmunoResarch	111-095-144	1:400
Fluorescein isothiocyanate anti-mouse	Goat	Jackson ImmunoResarch	115-095-062	1:400
Rhodamine red	Goat	Jackson	115-295-062	1:400

anti-mouse		ImmunoResarch		
Cy5 anti-rabbit	Goat	Jackson ImmunoResarch	111-175-144	1:400

The protocol followed in immunofluorescences is shown below:

1) Samples were rinsed in 1ml PBS for 6 changes, 5 min each, to eliminate OCT at room temperature.
2) At room temperature, slides were incubated 1 hour in blocking buffer,10% normal goat serum (Sigma-Aldrich, St. Louis, USA), 0,01% Triton X-100 (Panreac, Barcelona, Spain) in PBS. It blocked non-specific bounds and permeabilized cellular membranes to allow the entrance of antibodies.
3) Primary antibody (Ab) in blocking buffer was added in its correspondent dilution showed in **Table 2**. The incubation was at 4ºC overnight.
4) 3 washes at room temperature in PBS, eliminating the unbound primary Ab.
5) Incubation in secondary Ab during 1 hour at room temperature, under the minimum light condition to avoid the loss of fluorescence. The dilution used was the proper one showed in **Table 2**.
6) 3 washes at room temperature in PBS, eliminating the unbound secondary Ab.
7) Olfactory bulb sections were coverslip using Mowiol mounting medium (Sigma-Aldrich, St. Louis, USA).
8) When the samples were dried, they were observed and analyzed with a fluorescence microscope (Confocal Leica microscope TCS SP5 AOBS and Fluorescence Nikon microscope H6000L).

5.7. Microscopy and quantifications

5.7.1. Glomeruli quantification, glomeruli and IPL size measure

Glomeruli, in the GL, and IPL were visually identified in 5-6 sections of a 10th serie in each experimental mouse. Sections were located along the OB (3,56 to 5 mm from Bregma), and selected by similarity and position according to Paxinos' Atlas (Paxinos & Franklin, 2004)

after Nissl staining. Having selected the proper slices, images were taken with a Leica microscope TCS SP5 AOBS using the 10× objective and LAS V3.4.0 software.

Analysis under ImageJ 1.48v; Java 1.6.0_20 [64-bit] software were used to calculate total number of glomeruli, their area, and also the IPL area. This process consists in a visual identification of neurons over the digitized images and drawing the outline of glomeruli and IPL structures. A selected length of GL were used to standardized and compare the values in order avoid deviations due to OB size.

The arithmetic media was applied between four *Arx* mutants and six wild type mice. Statistical comparison was made using Student's unpaired t-test. For clarity, all the results were expressed as means ± s.e.m in column graphs. The level of significance was set at $P<0.05$ in all cases, with a two-tailed test. All statistical analyses were run on GraphPad Prism4 (San Diego, California, USA).

5.7.2. Quantification of OB neuronal subtypes

Each kind of neuron was identified by their localization and positive signal of specific antibodies against its markers. In each individual, 5-6 sections of a 10th series located along the OB (3,56 to 5 mm from Bregma), and selected by similarity and position according to Paxinos' Atlas (Paxinos & Franklin, 2004), were analyzed after immunofluorescence. Once the slices were selected, overlapping images were taken from each section with a Nikon H6000L fluorescence microscope and Leica microscope TCS SP5 AOBS using the 10× objective, NIS and LAS AF software.

The analysis of the pictures were developed using ImageJ 1.48v; Java 1.6.0_20 [64-bit] software to calculate total numbers throughout a selected length of the correspondent layer, in this way, all the values were standardized and able to compare. This process consists in a manual neuron identification over the digitized images, scoring in this case a minimum of 67 cells in one slice.

To compare the neuron number in each genotype, an arithmetic media was applied between four *Arx* mutants and seven wild type mice. Statistical comparison was made using Student's unpaired t-test. For clarity, all the results were expressed as means ± s.e.m in column graphs.

The level of significance was set at $P<0.05$ in all cases, with a two-tailed test. All statistical analyses were run on GraphPad Prism 4 (San Diego, California, USA).

RESULTS

6. RESULTS

6.1. Nissl staining

In order to obtain a general view of the OB structure in *Arx*$^{(GCG)}_{7}$ mutants and correspondent wt mice we performed a Nissl staining. Observations of the stained layers reveled differences between wt and *Arx*$^{(GCG)}_{7}$ mutants in the GL and IPL, so we proceed to further analyze the number of glomeruli, also their size and, finally, the width of the IPL.

6.1.1. Quantification of glomeruli

To examine whether glomeruli number was affected by *Arx*$^{(GCG)}_{7\ \text{mutation}}$, we performed a quantification of glomeruli in the GL from coronal sections of wt and *Arx*$^{(GCG)}_{7}$ mice, aged between 17 and 21 days. No significant difference were detected in the number of glomeruli between experimental groups (**Figure 3**), since the statistical study present a p value higher than 0.05 (P=0.1251, T=1.713, df=8, t-test). This data showed a media of 16.00±0.7 glomeruli (media±s.e.m.) in n=6 wild type mice, and 14.21±0.7 glmeruli (media±s.e.m.) in n=4 mutants.

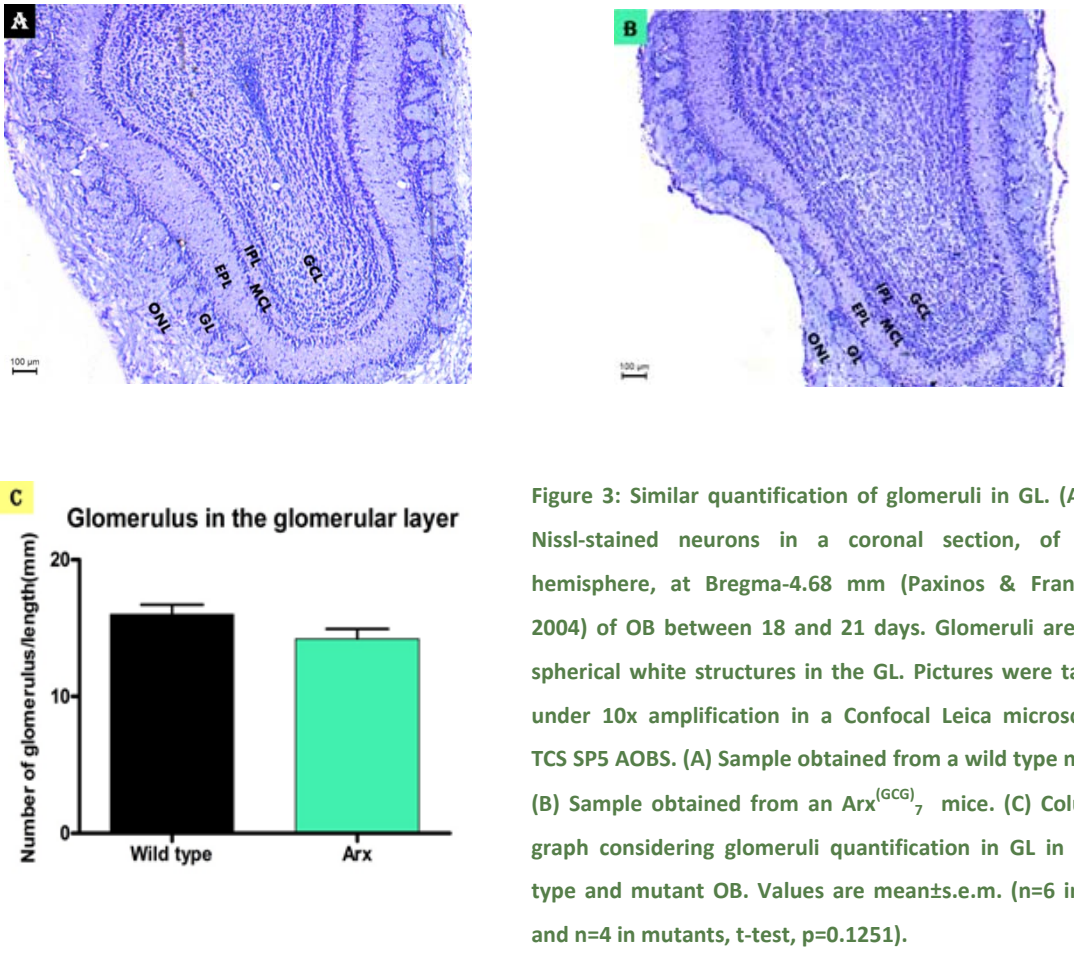

Figure 3: Similar quantification of glomeruli in GL. (A, B) Nissl-stained neurons in a coronal section, of one hemisphere, at Bregma-4.68 mm (Paxinos & Franklin, 2004) of OB between 18 and 21 days. Glomeruli are the spherical white structures in the GL. Pictures were taken under 10x amplification in a Confocal Leica microscope TCS SP5 AOBS. (A) Sample obtained from a wild type mice. (B) Sample obtained from an Arx$^{(GCG)}_{7}$ mice. (C) Column graph considering glomeruli quantification in GL in wild type and mutant OB. Values are mean±s.e.m. (n=6 in wt and n=4 in mutants, t-test, p=0.1251).

6.1.2. Size of glomeruli

To continue with the detailed structure study of glomeruli, their area were measured standardizing the results respect the length in which glomeruli were quantified (**Figure 4**). Glomeruli of *Arx*$^{(GCG)}_{7}$ mice (**Fig. 4B**) displayed a size reduction respect the wt mice (**Fig. 4A**) statistically significant *P=0.0178 (T=2.522, df=8, t-test). The mean size was of 3.188±0.1430 µm (media±s.e.m.) in n=6 wild type mice and 2.553±0.2243 µm (media±s.e.m.) in n=4 mutants (**Fig. 4C**). This approximately represents a 20% size reduction.

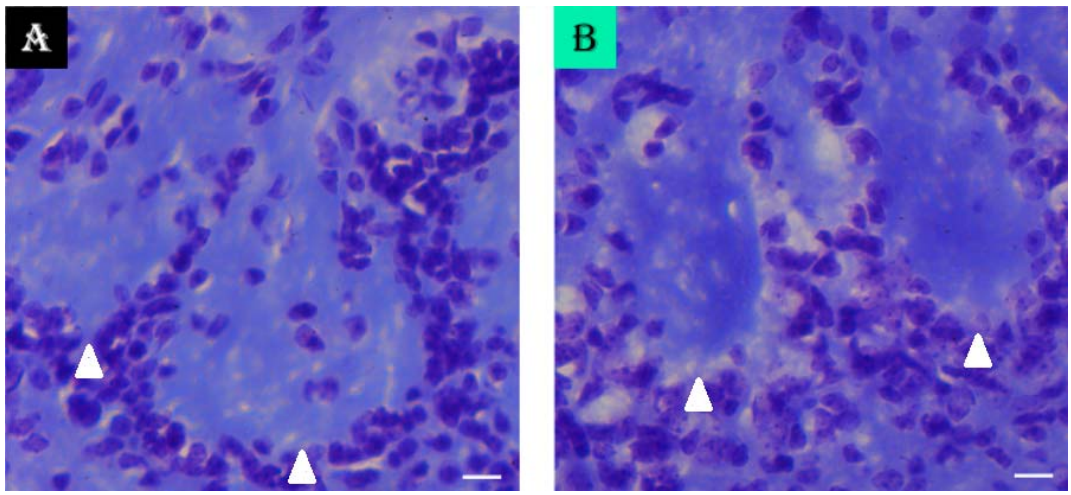

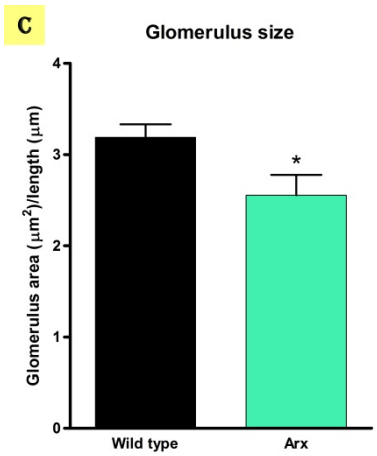

Figure 4: Size reduction of glomeruli in the OB in *Arx*$^{(GCG)}_{7}$ mice. (A, B) Nissl-stained neurons in a coronal section, of one hemisphere, at Bregma-4.68 mm (Paxinos & Franklin, 2004) **of 17-21 days old OB. Glomeruli are the spherical white structures in the GL. Pictures were taken under 40x amplification in a Confocal Leica microscope TCS SP5 AOBS. (A) Sample obtained from a wild type mice. (B) Sample obtained from an *Arx*$^{(GCG)}_{7}$ mice. (C) Column graph considering glomeruli area in GL in wt and mutant OB. Values are mean±s.e.m. (n=6 in wt and n=4 in mutants, t-test, *P=0.0178). Head arrows point glomeruli. Scale bar: 20µm.**

6.1.3. Size of IPL

Under the global view of Nissl staining, another difference that seems to exist between the mutant and the wt mice was the width of the IPL. Thus, it was histologically analyzed on coronal sections of wt (**Fig. 5A**) and *Arx*$^{(GCG)}_{7}$ mice (**Fig. 5B**). The latter displayed around a 70% size reduction of the IPL (value standardized respect the length in which the area data was obtained) at 17-21 days of age. Statistically the results represent a significant difference of ***P<0.0001 (T=8.188, df=8, t-test). At the same time the statistical study provides us with

the media: 35.84±1.887 µm (media±s.e.m.) in n=6 wild type mice and 10.58±2.515 µm (media±s.e.m.) in n=4 mutants (**Fig. 5C**).

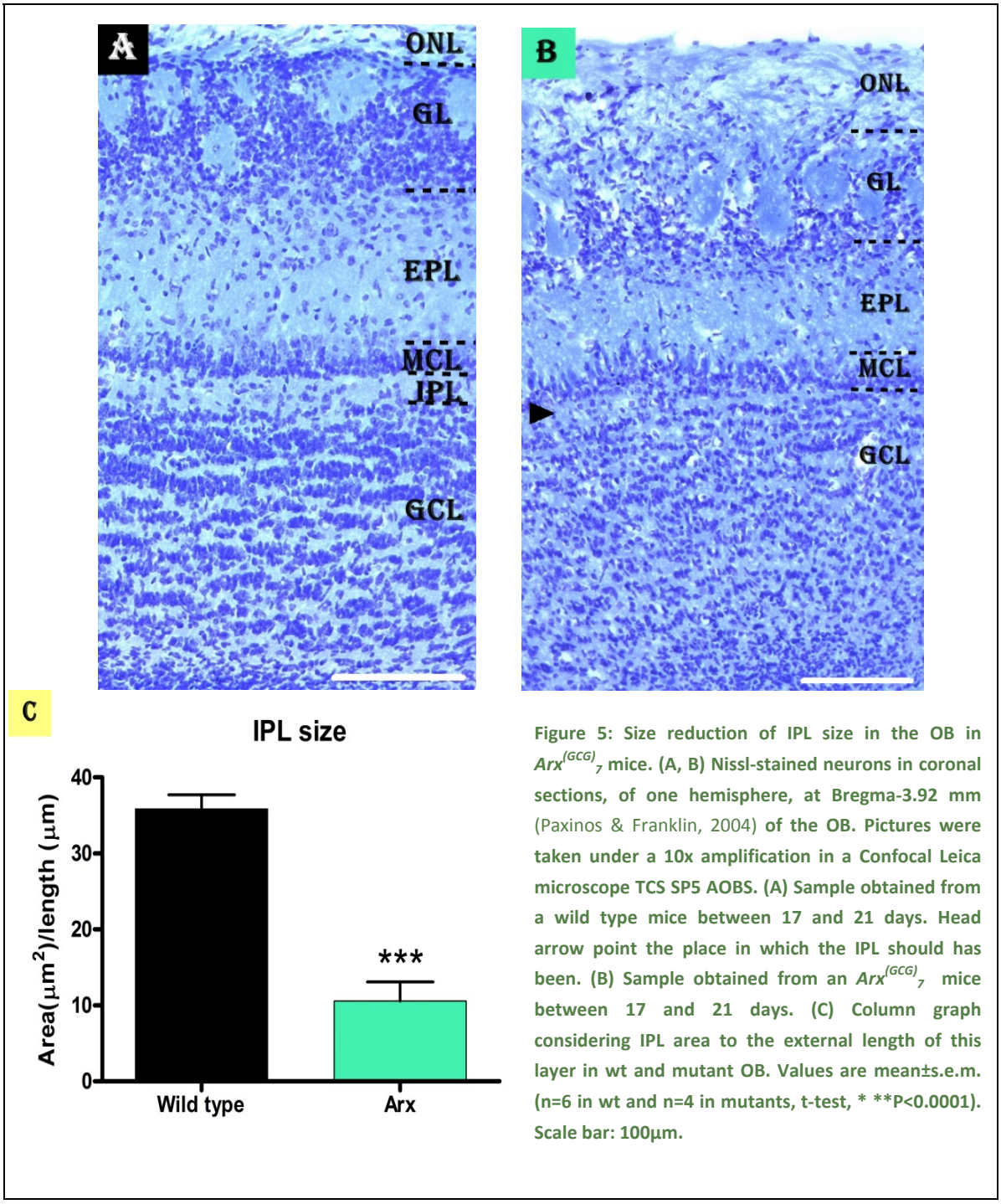

Figure 5: Size reduction of IPL size in the OB in *Arx*$^{(GCG)}_{7}$ mice. (A, B) Nissl-stained neurons in coronal sections, of one hemisphere, at Bregma-3.92 mm (Paxinos & Franklin, 2004) **of the OB. Pictures were taken under a 10x amplification in a Confocal Leica microscope TCS SP5 AOBS. (A) Sample obtained from a wild type mice between 17 and 21 days. Head arrow point the place in which the IPL should has been. (B) Sample obtained from an *Arx*$^{(GCG)}_{7}$ mice between 17 and 21 days. (C) Column graph considering IPL area to the external length of this layer in wt and mutant OB. Values are mean±s.e.m. (n=6 in wt and n=4 in mutants, t-test, * **P<0.0001). Scale bar: 100µm.**

6.1.4. Analysis of Calbindin^{+} (Cb^{+}) cell population

To further analyze the putative anomalies in cell distribution and differentiation that may occur in *Arx*$^{(GCG)_7}$ mice, we performed immunohistochemistry against specific marker of OB cellular sub-populations. First, we detected one of the main PG interneuron populations, using anti-Cb antibody on coronal sections of *Arx*$^{(GCG)_7}$ and wt OB. Results showed a statistically signicant reduction in *Arx*$^{(GCG)_7}$ (**Fig. 6B**) versus wt mice (**Fig. 6A**) (***P<0.0001 (T=7.681 df=9)). This data presented a media of 95.39±4.777 cells/mm (media±s.e.m.) in n=7 wild type mice and 44.40±2.066 cells/mm (media±s.e.m.) in n=4 mutants (**Fig. 6C**). No differences were observed in distribution and location of the Cb$^+$ cells between experimental groups. Interestingly, we observed a reduction in the intensity of the Cb signal in the mutant mice. This suggests a control of Cb gene expression by the ARX transcription factor that is affected by the mutation.

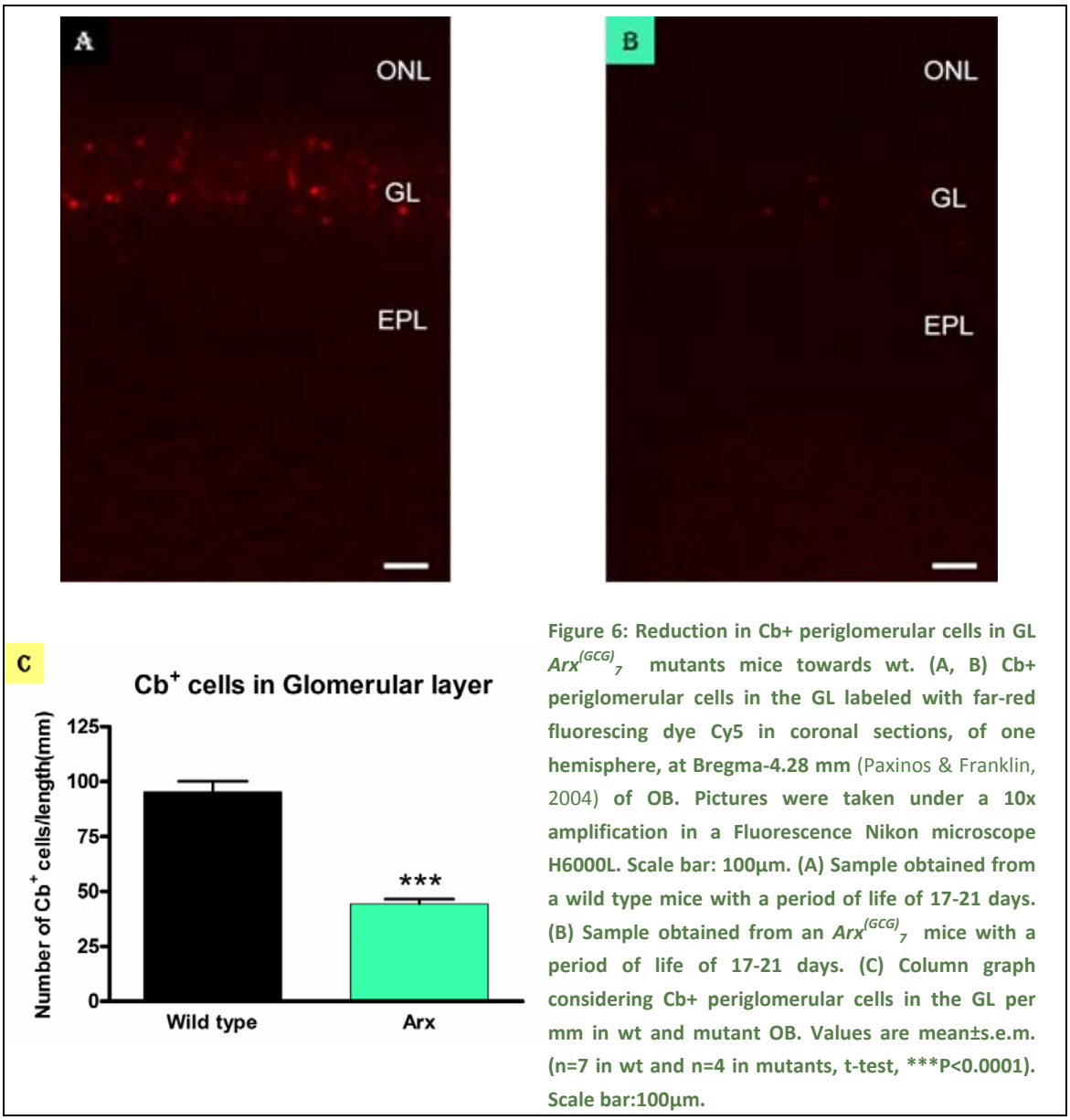

Figure 6: Reduction in Cb+ periglomerular cells in GL *Arx*$^{(GCG)_7}$ mutants mice towards wt. (A, B) Cb+ periglomerular cells in the GL labeled with far-red fluorescing dye Cy5 in coronal sections, of one hemisphere, at Bregma-4.28 mm (Paxinos & Franklin, 2004) **of OB. Pictures were taken under a 10x amplification in a Fluorescence Nikon microscope H6000L. Scale bar: 100µm. (A) Sample obtained from a wild type mice with a period of life of 17-21 days. (B) Sample obtained from an *Arx*$^{(GCG)_7}$ mice with a period of life of 17-21 days. (C) Column graph considering Cb+ periglomerular cells in the GL per mm in wt and mutant OB. Values are mean±s.e.m. (n=7 in wt and n=4 in mutants, t-test, ***P<0.0001). Scale bar:100µm.**

6.1.5. Analysis of Calretinin$^+$ (CR$^+$) cell population

Finally, to characterize the third periglomerular interneuron population in the GL we performed immunohistochemistry using anti-CR antibody on coronal sections of *Arx*$^{(GCG)_7}$ and wt mice. CR is also expressed in the GCL and detect interneurons during migratory process. At 17-21 days, there was no significant difference in the number of CR+ cells in the PG layer (**Figure 7**), because p value was 0.3444 (T=1.044, df=5, t-test). This data showed a media of 243.7±12.90 cells/mm (media±s.e.m.) in n=5 wild type mice and 219.1±17.79 cells/mm (media±s.e.m.) in n=2 mutants. No differences were observed in distribution and location of the CR$^+$ cells between experimental groups in other cell layers (data not shown).

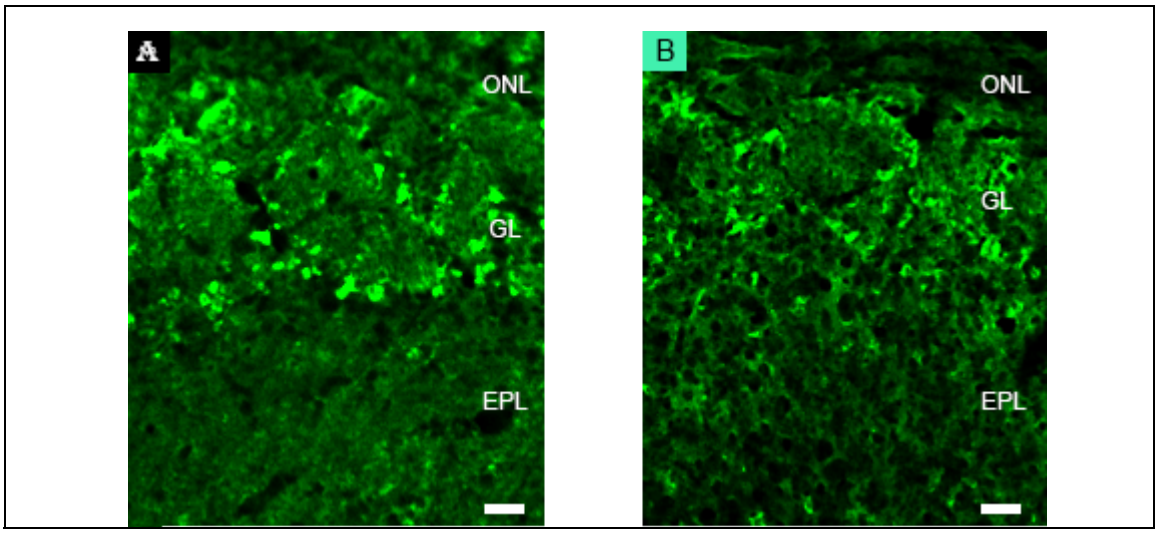

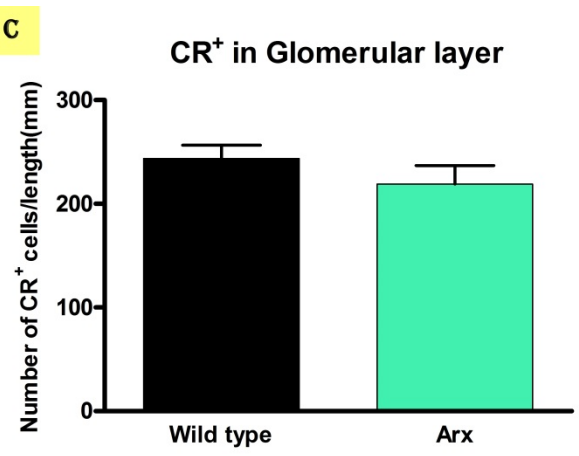

Figure 7: Similar CR+ periglomerular cells in GL *Arx*$^{(GCG)}_{7}$ mutants and wt mice. (A, B) CR+ periglomerular cells in the GL labeled with red fluorescing dye Rhodamine Red in coronal sections, of one hemisphere, at Bregma-4.28 mm (Paxinos & Franklin, 2004) **of 17-21 days OB. Pictures were taken under a 10x amplification in a Fluorescence Nikon microscope H6000L. (A) Sample obtained from a wild type mice. (B) Sample obtained from an *Arx*$^{(GCG)}_{7}$ mice. (C) Column graph considering CR+ periglomerular cells in the GL per mm in wt and mutant OB. Values are mean±s.e.m. (n=5 in wt and n=2 in mutants, t-test, p=0.3444). Scale bar: 100µm.**

6.1.6. Analysis of Tyroxine Hydroxylase (TH+) cell population

To characterize the second main population of periglomerular cells, we performed immunohistochemistry using anti-TH antibody on coronal sections of *Arx*$^{(GCG)}_{7}$ and wt mice (**Fig. 8A, 8B**). A remarkable difference existed between TH^{+} cells in 17-21 days *Arx*$^{(GCG)}_{7}$ and wt mice, ** P= 0.0043 (T=3.787, df=9, t-test). This data showed a media of 28.42±2.092 cells/mm (media±s.e.m.) in n=7 wild type mice and 15.76±2.455 cells/mm (media±s.e.m.) in n=4 mutants (**Fig. 8C**). No differences were observed in localization of the TH^{+} cells between experimental groups.

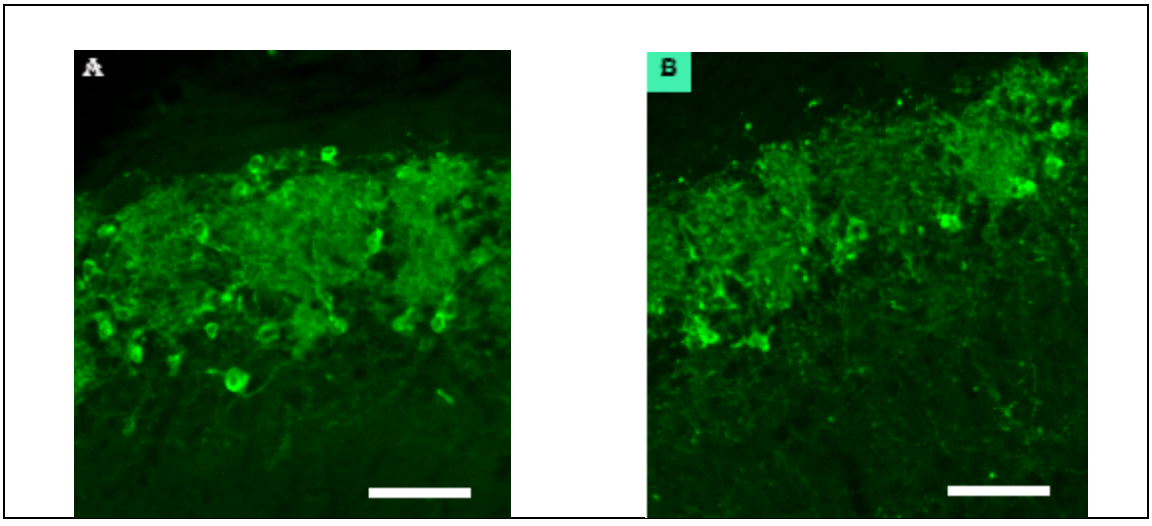

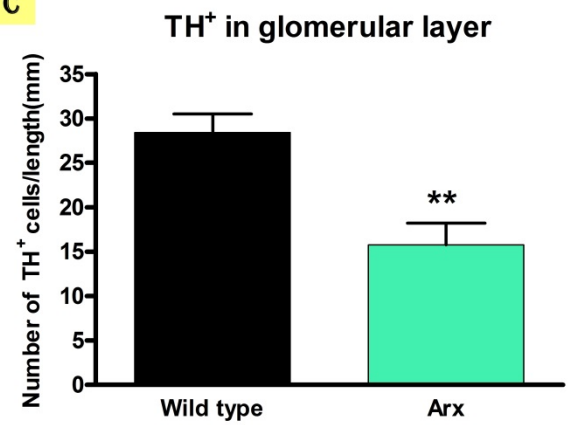

Figure 8: Reduction in TH+ periglomerular cells in GL *Arx*$^{(GCG)}_{7}$ mutants mice towards wt. (A, B) TH+ periglomerular cells in the GL labeled with red fluorescing dye Rhodamine Red in coronal sections, of one hemisphere, at Bregma-4.28 mm (Paxinos & Franklin, 2004) **of 17-21 days OB. Pictures were taken under a 10x amplification in a Fluorescence Nikon microscope H6000L. (A) Sample obtained from a wild type mice. (B) Sample obtained from an *Arx*$^{(GCG)}_{7}$ mice. (C) Column graph considering TH+ periglomerular cells in the GL per mm in wt and mutant OB. Values are mean±s.e.m. (n=7 in wt and n=4 in mutants, t-test, **P=0.0043). Scale bar: 250µm.**

6.1.7. Analysis of Reelin+ cell population

To determine whether the signal of tangential migration was established in *Arx*$^{(GCG)}_{7}$ mutants, and to analyze the morphology, number and distribution of mitral cells we performed an immunohistochemistry against Reelin in coronal sections of wt and *Arx*$^{(GCG)}_{7}$ OB (**Fig. 9A, 9B** respectively). In a period of 17-21 days of mice's life, there was no significant difference in the number of Reelin^{+} cells between Arx$^{(GCG)}_{7}$ and wt mice, P= 0.7996 (T=0.2615, df=9, t-test). This showed a media of 66.36±4.452 cells/mm (media±s.e.m.) in n=7 wild type mice and 64.54±4.893 cells/mm (media±s.e.m.) in n=4 mutants (**Fig. 9C**). No alterations in the monocellular layer distribution and reelin expression was observed between groups.

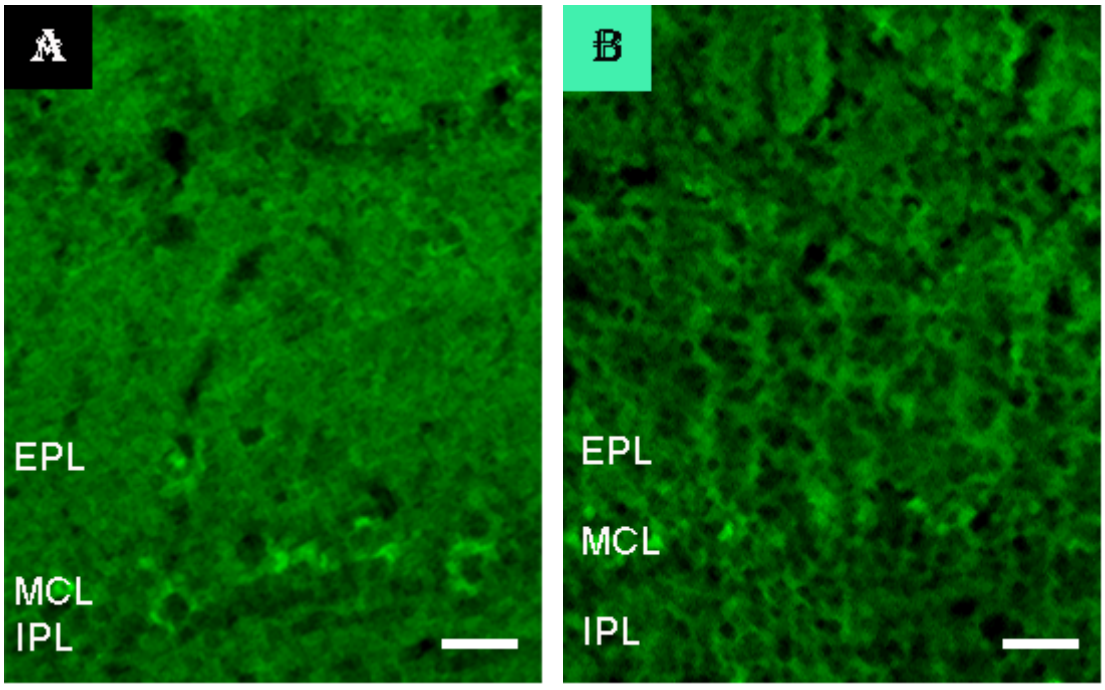

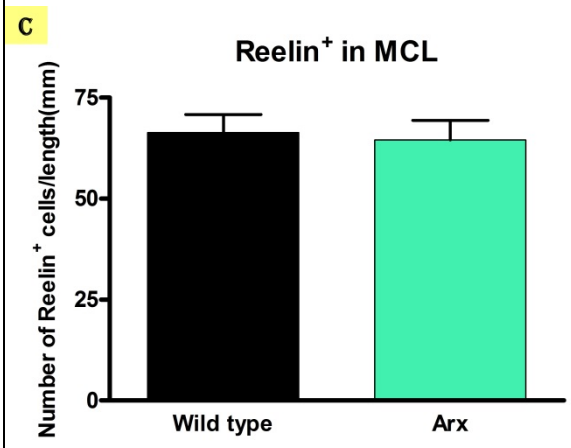

Figure 9: Similar Reelin+ mitral cells in MCL *Arx*$^{(GCG)}_{7}$ mutants mice towards wt. (A, B) Reelin+ mitral cells in the MCL labeled with green fluorescing dye FITC (Fluorescein Isothiocyanate) in coronal sections, of one hemisphere, at Bregma-4.28 mm (Paxinos & Franklin, 2004) **of OB. Pictures were taken under a 10x amplification in a Fluorescence Nikon microscope H *Arx*$^{(GCG)}_{7}$ mice between 17 and 21 days of life. (C) Column graph considering Reelin+ mitral cells in the MCL per mm in wt and mutant OB. Values are mean±s.e.m. (n=7 in wt and n=4 in mutants, t-test, p=0.7996). Scale bar: 100µm.**

DISCUSSION

7. Discussion

To date, the function of *Arx* gene in the OB has just been analyzed in KO mice by Yoshihara et al., which does not reflect anomalies in living adult animals due to the lethality of *Arx-KO* mutation. At the same time, it doesn't represent any born alive human phenotype or relation to a known pathology, because of the same reason. However, it provides relevant data about the role of this gene in the OB development and morphology. Taking into account these antecedents, this project was focused on the study of the *Arx* mutation c.304ins(GCG)7 which represents the most common cause of a human infantile epilepsy denominated WS. Thus, not only the phenotype in the OB is observed in order to project the results in humans, understanding better this disease. But also, with this mutation a lower expression and activity of Arx protein is simulated in young mice, gaining knowledge about the biological repercussion in the OB formation. Compiling the results obtained in the previous KO study and in this project with the *Arx*$^{(GCG)}_{7}$ mutation, a clear understanding of Arx gene function in the OB is acquired, presenting a unquestionable role in its structural configuration. Below, a complete detailed analysis of the results will be made.

Starting with Nissl staining, we determine that the number of glomeruli is preserved in the mutants as in the wt mice. In contrast, their size is significantly reduced. Since glomeruli constitute a spherical structure form by the terminals of the olfactory nerve and the dendrites of mitral, periglomerular and tufted cells; the decrease in size could be a consequence of one or several of the following points:

- A higher compacting of these terminals and dendrites.
- A reduction in one or more types of the cells that form it (mitral, periglomerular or tufted cells).
- A decrease in the number of terminals of the olfactory nerve.
- An inclusion of periglomerular somata cells in the glomeruli.

Considering that after having made immunofluoresce analysis against Reelin, a mitral cell marker, no mayor alterations was observed in distribution and number, we may conclude that they will not be involved in the glomeruli size reduction. However, we should notice that just somata was labeled with this antibody, being possible that dendrites could be reduced while the number of cells remained stable. For this reason, further studies labeling dendrites would

be useful to discard any implication of the mitral cells in this alteration. Furthermore, it will provide us with an answer to the other previously cited hypothesis: whether there is a more compacting structure and fewer terminals. To label olfactory nerve fibers assays, such as response to chemical stimuli by capsaicin, could be developed and determine their presence in glomeruli (Silver et al., 1994; Yoshihara et al., 2005).

The reduction in mitral cell number was discarded. However, according to periglomerular cell analysis by immunofluorescence we can conclude that TH positive cells are reduced in *Arx*$^{(GCG)}_{7}$ mice comparing to wt. This may contribute to the reduction in size of the glomeruli. On the other hand, in the KO mice their signal disappeared completely in the OB, so if we join our results with the studies followed by Yoshihara et al., their hypotheses could be complemented. *Arx* gene may be located upstream of Nurr1 and TH genes in a genetic cascade for their correct differentiation, presenting a poor activation with the low expression of *Arx* gene (*Arx*$^{(GCG)}_{7}$). The other possibility is that the progenitors of TH(+) OB interneurons may not be exposed to appropriate differentiation signals produced in the OB due to the impaired entry into the OB (Yoshihara et al., 2005). We should perform further experiments to verify wether TH+ cell reduction is due to deficits in the migration or in their generation. Among them it would be useful to study migration with BrdU or the proliferation with k167 which label cells in division or PCNA that is a marker of division cells in a latter phase (Ang et al., 2006; Jalava et al., 2006; Strzalka & Ziemienowicz, 2011; Yoshihara et al., 2005).

We have extended more in detail the analysis of other PG interneuron populations with the Cb and CR staining. These two protein markers were not studied in KO mice:

- Calbindin(+) periglomerular cell number also present a high reduction in *Arx*$^{(GCG)}_{7}$ mice. So, a hypothesis is that *Arx*$^{(GCG)}_{7}$ mutation plays a repression role in the development, generation or migration of this cell type. Further studies should be performed, however the downregulation in the signal of Cb observed in the *Arx*$^{(GCG)}_{7}$ suggest a direct effect of this gene on the signal cascade for their correct differentiation. Nonetheles, experiments with a pulse of BrdU will help to clarify the different hypothesis.
- Calretinin(+) periglomerular cells did not displayed a difference in number, being compared to wt mice. As a result, Arx gene could not be involved in the correct development and disposition of this kind of cels in the OB or, on the other hand, with a low

activity and quantity of Arx protein CR(+) interneurons follow its normal phenotype behavior.

Indicate that the anomaly in glomeruli size was magnified in KO mice, more especifically, protoglomeruli structures were only observed in wild type. Before 10 postnatal days, glomeruli do not yet exist. Until this moment, they will present protoglomeruli, where mitral cells initially receive synatic input from these structural compartments, and with time mitral cell primary dendritic fields regress, so that only one or a few glomeruli are innervated, and secondary dendrites emerge from the region of the cells soma. It is not yet discovered how this process is performed, but it seems that *Arx* plays a crucial role and with low expression of this factor will be enough to constitute the signal for the formation of a glomeruli, however, its size is altered due to deficits in the PG interneurons that we report in this work (Malun & Brunjes, 1996; Yoshihar et al., 2005).

Another main difference found with Yoshihara's study is centered in MCL. While with the complete deletion of the gene MCL was observed to be thicker and with irregular contour, in Arx$^{(GCG)}_7$ mice present the same structure and number of mitral cells.

Regarding the IPL it should be pointed out that in the previous study it was not observed because it is a harsh work to differentiate this layer before P0. In contrast, it is clearly established in P17-P21. Thus, its study was followed in this project with a remarkable difference between mutants and wt mice. The IPL reduced its width, resulting in a thinner layer. The total OB size is probably reduced cause of the almost total disappearance of this layer in mutants. The reason of the reduction could be due to a closer association of axons of mitral and tufted cells, the loss of some of those axons or their incorrect projection. In addition, cell migration defects may contribute to locate improperly cells in this layer and hide its real extension. As a way to determine which is the defect, further analysis should be held, among them it would be useful to study migration with BrdU pulses and perform staining of axonal projections with specific markers such as L1 or TAG-1.

It is also interesting to highlight that it should not be forgotten that we are studying just one gene in this work. However, mammals are known to be complex organism with a wide network of genes that correlate to achieve the correct functioning. So, even if Arx is

intrinsically involved in OB morphology, it could be interacting in conjunction with other genes. For example, Sp8 transcription factor has been proved to impair the general cytoarchitecture of the mutant OB. Mutants of that gene present similarities with our *Arx* mutant mice. As *Arx* homeobox protein, Sp8 is not found in the projection neurons. Furthermore, both mutations exhibit severe reductions in the volume of interneurons, indicating that interneurons contribute importantly to the cytoarchitectural organization of the forming OB.

To finish, regarding to the odor perception in mutants it would be of interest to do behavioural tests in mice in order to study possible alterations. Nevertheless, tests with this young-aged mice is difficult to perform, since individuals are lactant until day 15 of life, at least, narrowing the temporal window to do behavioral assays. It would be of interest to search clinical antecedents in WS patient to find deficits in odor perception that could confirm the relevance of Arx mutation in the human OB formation.

CONCLUSIONS

8. CONCLUSIONS

1. . Arx gene is necessary for the correct Glomeruli and IPL development in the OB.
2. Arx$^{(GCG)}_{7}$ mutation affects the number of specific types of OB interneurons: Cb^{+}and TH^{+} periglomerular cells in the GL.
3. Deffects in glomeruli size are likely due to the reduction in the number of Cb^{+}and TH^{+} periglomerular interneuron populations.
4. The results suggest a possible defect in OB and odor perception in patients with WS.

REFERENCES

7, REFERENCES

Beguin, S., Crépel, V., Anikszteјn, L., Becq, H., Pelosi, B., Pallesi-Pocachard, E., et al. (2012). An epilepsy-Related ARX Polyalanine Expansion Modifies Glutamatergic Neurons Excitability and Morphology Without Affecting GABAergic Neurons Development. *Cerebral Cortex*. 23(6):1484-94.

Crespo, C., Liberia, T., Blasco-Ibáñez, J., Nácher, J., & Varea, E. (2003). The Circuits of the Olfactory Bulb.The Exception as a Rule. *The Anatomical Record*, 296(9): 1401-1412.

Engel JR, J., & Pedley, T. (2008). Preface to the First Edition. En J. Engel JR, & T. Pedley, *Epilepsy a comprehensive textbook (Volume three)* (pág. xli). Philadelphia: Lippincott Williams & Wilkins, a Wolters Kluwer Business.

Gécz, J., Cloosterman, D., & Partington, M. (2006). ARX: a gene for all seasons. *Current Opinion in Genetics & Development*, 16(3):308-316.

Jalava, P., Kuopio, T., Juntti-Patinen, L., Kotkansalo, T., Kronqvist, P. & Collan, Y. (2006). Ki67 immunohistochemistry: a valuable marker in prognostication but with risk of misclassification: proliferation subgroups formed based on ki67 immunoreactivity and standardized mitotic index. *Histopathoogy*, 48(6): 674-682.

Kato, M. (2006). A new paradigm for West syndrome based on molecular and cell biology. En P. Schwartzkroin, *Encyclopedia of Basic Epilepsy Research* (págs. S87-S95). Academic Press.

Lledo, P.-M., Gheusi, G., & Vincent, J.-D. (2005). Information Procesing in the Mammalian Olfactory System. *Physiological Reviews*, 85(1):281-317.

Malun, D. & Brunjes, P.(1996). Development of Olfactory Glomeruli: Temporal and Spatial Interactions between Olfactory Receptor Axons and Mitral Cells in Opossums and Rats. The Journal of Comparative Neurology, 368(1):1-16.

Mori, k., Nagao, H., & Yoshihara, Y. (1999). The Olfactory Bulb: Coding and Processing of Odor Molecule Information. *Science*, 286(5440):711-5.

NCBI. (2014, April 8). Retrieved April 26, 2014, from http://www.ncbi.nlm.nih.gov/gene/170302#bibliography

Pahle, J., Valova, I., & Georgiev, N. (June 2000). Oscillatory Simulation of Mitral and Granule Cell Behavior in the Olfactory Bulb. *International Conference on Artificial Intelligence (IC-AI'2000).*

Pancoast Nasrallah, M., Cho, G., Simonet, J., Putt, M., Kitamura, K., & Golden, J. (2011). Differential effects of a polyalanine tract expansion in Arx on neural develpent and gene expression. *Human Molecular Genetics*, 21(5): 1090-1098.

Paul Eling, W. O. (2002). The mystery of the Doctor's son, or the riddle of West syndrome. *Neurology*, 58:6:953-955.

Paxinos, G., & Franklin, K. (2004). *The mouse Brain in stereotaxic coordinates.* USA: ElSevier Academic Press.

Shorvon, S. (2009). Definition and frequency of epilepsy. En S. Shorvon, *Epilepsy* (pág. 1). New York: Oxford Neurology Library.

Silver, W., Thomas, F., & Bärbel, B. (1994). Nasal Trigeminal Chemoreceptors May Have Affect and Effector Functions. *27th Japanese Symposium on Taste and Smell*, (pág. 322). Sapporo (Japan).

Strzalka, W. & Ziemienowicz, A. (2010). Proliferating cell nuclear antigen (PCNA): a key factor in DNA replication and cel cycle regulation. *Annals of Botany,* 107(7): 1127-1140.

Waclaw, R., Allen , Z., Bell, S., Erdélyi, F., Szbó, G., Potter, S., y otros. (2006). The Zinc Finger Transcription Factor Sp8 Regulate the Generation and Diversity of Olfactory Bulb Interneurons. *Cell*, 49(4): 503-516.

Wheless, J., Gibson, P., Rosbeck, K., Hardin, M., O'Dell, C., Whittemore, V., et al. (2012). Infantile spasms (West syndrome): update and resources for pediatricians and providers to share with parents. *BMC Pediatrics*, 12:108.

Yoshihara, S.-I., Omichi, k., Yanazawa, M., Kitamura, k., & Yoshihara, Y. (2005). Arx homeobox gene is essential for development of mouse olfactory system. *Development*, 132(4): 751-762.

Zou, D.-J., Chesler, A., & Firestein, S. (2009). How the olfactory bulb got its glomeruli: a just so story? *Nature Reviews*, 10(8):611-618.

LIST OF ILUSTRATIONS

9. LIST OF ILUSTRATIONS